

Testing time order and Leggett-Garg inequalities with noninvasive measurements on public quantum computers

Tomasz Rybotycki^{1,2,3}, Tomasz Białcki^{4,5}, Josep Batle^{6,7}, Bartłomiej Zglinicki⁴, Adam Szereszewski⁴, Wolfgang Belzig⁸, and Adam Bednorz⁴

¹*Systems Research Institute, Polish Academy of Sciences, ul. Newelska 6, 01-447 Warsaw, Poland*

²*Nicolaus Copernicus Astronomical Center, Polish Academy of Sciences, ul. Bartycka 18, 00-716 Warsaw, Poland*

³*Center of Excellence in Artificial Intelligence, AGH University, al. Mickiewicza 30, 30-059 Cracow, Poland*

⁴*Faculty of Physics, University of Warsaw, ul. Pasteura 5, PL02-093 Warsaw, Poland*

⁵*Faculty of Physics and Applied Informatics, University of Lodz, ul. Pomorska 149/153, PL90-236 Lodz, Poland*

⁶*Departament de Física and Institut d'Aplicacions Computacionals de Codi Comunitari (IAC3), Campus UIB, E-07122 Palma de Mallorca, Balearic Islands, Spain*

⁷*CRISP – Centre de Recerca Independent de sa Pobla, 07420 sa Pobla, Balearic Islands, Spain and*

⁸*Fachbereich Physik, Universität Konstanz, D-78457 Konstanz, Germany*

We present two protocols, with one and two two-qubit gates, to noninvasively measure two incompatible observables on a qubit. Both protocols are completed with a projective measurement. By gathering sufficiently large statistics, we have been able to violate Leggett-Garg inequality and time-order invariance. The detailed analysis of the data on 10 qubit sets from 5 devices available on IBM Quantum and one on IonQ reveals violations beyond 5 standard deviations in almost all cases. We implemented our protocols using fractional gates, newly available on the IBM Heron devices, allowing us to benchmark them in application to weak measurements. The noninvasiveness is supported by a qualitative and quantitative agreement with the model of weak disturbance. These results show another characteristic feature of quantum measurements.

I. INTRODUCTION

Quantum physics defies classical intuitions, most prominently in the violation of local realism [1–3]. The root of many nonclassical properties is that the values of the observables do not exist before measurement — they are probabilistic [4]. The problem occurs for incompatible observables, which are expressed formally by noncommuting operators. Attempts to define the values of incompatible observables, even when not measured, always end up with a disagreement with some classical expectation. For example, Wigner function could be the joint probability of incompatible position and momentum, but it is negative in specific cases [5]. On the other hand, one cannot constantly apply a projective measurement as it freezes systems' dynamics (so called quantum Zeno effect [6]). An incompatible projective measurement disturbs further evolution, e.g. in Elitzur-Vaidman bomb [7, 8]. Another long-standing conflict with quantum reality is violation of Leggett-Garg (LG) inequality [9, 10], under the assumption of noninvasiveness and macrorealism. In its original form, LG inequality shows that strong, projective measurements [11] violate these assumptions. This claim was shown in numerous experiments [12, 13]. Since projective measurements seem to be highly invasive, their outcomes cannot reveal realistic properties of a quantum system.

A partial solution is measuring not projectively, but with a finite strength. The smaller the strength, the better. It can be done by adding an interaction with an auxiliary detection space, equivalent to a positive operator-valued measure (POVM) [14–17]. Such a measurement leads to a balance between accuracy and disturbance. In time-continuous version, the measure-

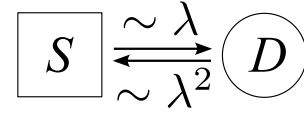


FIG. 1. The scheme of weak measurement. The system S interacts with the ancillary detector D which gains information from the weakly-measured system scaled by the measurement strength λ , while causing disturbance to the system of the order λ^2 .

ment causes a collapse, becoming effectively a projection, within the timescale depending on the measurement strength [18, 19]. The POVM is noninvasive only if it's commuting with all the relevant observables, e.g. identity [20].

The strongest candidate for a genuine noninvasive measurement is the so-called weak measurement. It's modeled so that it has small strength and disturbance [21]. In the weak measurement scheme, the auxiliary detector gains information from the weakly-measured system in a form of an additional signal on top of the device noise, scaled by the measurement strength. The latter is meant to be small. Notice that in this scenario the disturbance of the weakly measured system is also weak, as it scales with the square of the measurement strength, see Fig. 1.

Weak measurements remain in conflict with restrictions following from classical realism. Their averages exceed the projective limits [22–26] and violate LG inequalities by a combination of correlations in time [27–36]. The natural model of weak measurement [37, 38] leads to correlations depending on the time order of measurements [39], and violation of conservation of energy

and other classical invariants of motion in third order correlations [41]. The former issue has also been shown experimentally [40].

When the public quantum computers became available via IBM Quantum platform [42], experiments involving LG tests have been performed, although only in the version with projective measurements [44, 45]. IBM machines have also been shown to handle weak measurements [46]. In the hereby paper, we demonstrate violation of LG inequalities and time order symmetry using weak measurements. We run our experiments on publicly available quantum devices from IBM and IonQ. For the former, we used 4 different devices. We started with the simulations, during which we identified ten 3-qubit groups that were most likely to violate the LG inequalities. Each simulation was run with the noise model of a respective device. We then applied two protocols of weak measurements, one with a single and the latter with two standard two-qubit gates, including new fractional gates available on IBM Heron generation devices [47]. The results confirm LG and time-symmetry violation on most of the groups by 10 standard deviations on average. We have also checked that the measurement is indeed non-invasive, i.e. the correlations are different from the ones obtained by applying projective measurements. In the case of IonQ we have selected a single 3-qubit group on a single device. We also used a single entangling gate. Our choice was made due to all-to-all connectivity on the selected device.

The paper is organized as follows. First, we summarize the concept of weak measurements, LG inequalities and time order. Next, we describe the applied experimental protocol, using native qubit topology and gates of the IBM devices. Then, we present the results, commenting their most significant features. We finish with a discussion, stressing the pros and cons of our experiment. We also suggest further routes to test noninvasiveness and quantum realism even more convincingly.

II. WEAK MEASUREMENT

Suppose we have a generic POVM represented by Kraus operators $K(a)$ where a is the measurement outcome [14–17]. Then the state ρ becomes

$$\rho(a) = K(a)\rho K^\dagger(a) \quad (1)$$

with probability $p(a) = \text{Tr}\rho(a)$, and normalized by $\int da p(a) = 1$. In the case of null, completely noninvasive measurement, we expect an unchanged ρ , i.e.

$$\int da \rho(a) = \rho \quad (2)$$

A straightforward observation is that the only possibility to achieve it occurs when $K(a) = k(a)\mathbb{1}$ (scaled identity) for some a function $k(a)$, which is commonly referred to as no information gain without disturbance [20].

We shall denote classical and quantum averages $\langle f(a) \rangle \equiv \int da p(a)f(a)$ and $\langle F \rangle = \text{Tr}\rho F$, respectively. In the completely noninvasive case, the detector measures its own noise. Without loss of generality we assume that this noise is centered at 0 and has a definite finite variance $\langle a^2 \rangle$. We further assume that the information obtained from the system is encoded in the average $\langle a \rangle$. Then the following theorem, linking quantum state discrimination and disturbance, holds.

Theorem 1 *If there exist two states ρ_\pm in some Hilbert subspace \mathcal{H} such that $\Delta = \langle a \rangle_{\rho_+} - \langle a \rangle_{\rho_-}$, then there exists such a pure state $\rho \in \mathcal{H}$ that*

$$1 - \text{Tr}\rho' \rho \geq \Delta^2/4\sigma^2, \quad (3)$$

where $\rho' = \int da K^\dagger(a)\rho K(a)$ is the output state and σ^2 is the upper bound on the variance $\langle (a - \langle a \rangle)^2 \rangle$ in \mathcal{H} .

The proof is in Appendix A. The meaning of Δ is the ability of the measurement to discriminate between the states ρ_\pm due to the difference of the average of a . For pure states, ρ and ρ' , $\text{Tr}\rho' \rho$ is equal to the fidelity $F(\rho', \rho)$ defined in general as $\sqrt{F} = \text{Tr}\sqrt{\sqrt{\rho}\rho'\sqrt{\rho}}$ [17], and giving the lower bound on the Bures distance [48] $B^2 = 2(1 - \sqrt{F}) \geq 1 - F$, the trace distance $D(\rho, \rho') = \text{Tr}|\rho - \rho'|/2 \geq 1 - \sqrt{F}$, and Hilbert-Schmidt distance $\text{Tr}(\rho - \rho')^2 \geq (1 - F)^2$. The restriction on the subspace \mathcal{H} has two goals: (i) to ignore extremal states with artificially large Δ , (ii) to allow superpositions that can be otherwise forbidden e.g. by superselection rules [49]. The expression by fidelity allows experimentally determined discrimination, e.g. by measuring projection $B = \rho$. Applying the theorem to the case $a = \pm 1$, i.e. a measurement scheme with dichotomic discrimination, one can simply take $\sigma^2 = 1$. Identifying the average with an observable

$$A = \int da a K^\dagger(a)K(a) \quad (4)$$

is attractive (as $\langle A \rangle = \langle a \rangle$), but misleading. For instance, we do not necessarily have a measurement scheme to retrieve e.g. $\langle A^2 \rangle$. To this end, we should introduce a special family of measurements $K(a) = k(a, A)$ for a Hermitian operator A satisfying

$$\int da |k(a, A)|^2 = 1. \quad (5)$$

For instance, a Gaussian measurement

$$k(a, A) = (2\pi)^{-1/4} \exp(-(a - A)^2/4) \quad (6)$$

has the property $\sigma^2 = 1$ and

$$\langle a^2 \rangle = \langle A^2 \rangle + 1 \quad (7)$$

and in general the measurement probability is a convolution

$$p(a) = \int da' n(a - a') \langle \delta(a - A) \rangle \quad (8)$$

with the normal distribution $n(a) = (2\pi)^{-1/2} \exp(-a^2/2)$. The disturbance on a generic state ρ can be then described by

$$\rho' = \int da K(a) \rho K^\dagger(a) = \exp(-\mathcal{G}_A/8) \rho \quad (9)$$

where $\mathcal{G}_A \rho = [A, [A, \rho]]$ imposes decoherence – reduction of the off-diagonal elements of ρ in the eigenbasis of A . In particular, if $A = \int da |a\rangle\langle a|$ for the orthonormal basis of states $|a\rangle$ then

$$\langle \bar{a} | \rho' | a \rangle = e^{-(a-\bar{a})^2/4} \langle \bar{a} | \rho | a \rangle. \quad (10)$$

For a dichotomic scheme, with $a = \pm 1$ and

$$K(a) = \sqrt{(1 + aA)/2} \quad (11)$$

restricting $|A| \leq 1$, we get disturbance

$$2\rho' = \sqrt{1 + A\rho}\sqrt{1 + A} + \sqrt{1 - A\rho}\sqrt{1 - A}. \quad (12)$$

To get the variable-strength measurement we replace $A \rightarrow \lambda A$ with the constant parameter $\lambda > 0$. For $\lambda \rightarrow \infty$ in the Gaussian scheme ($\lambda \rightarrow 1$ in the dichotomic scheme with $A^2 = 1$) we obtain a strong, projective measurement, while $\lambda \rightarrow 0$ is the limit of weak measurement. As we have seen, there always is a disturbance. However, with introduction of λ , we get $\sim -\lambda^2 \mathcal{G}_A/8$ in (9), in agreement with our theorem. Hence, small λ justifies invasiveness. From the experimental point of view, there is no guarantee that the disturbance is small in the whole Hilbert space, including the apparently non-accessible part of the space. We have to trust the measurement scheme. This trust would be necessary in the classical picture, but there would not be a lower bound on the disturbance.

We emphasize that only the limiting behavior of weak measurements is important. To construct their general family, we shall look into the construction of POVM, expressing Kraus operators by elements of a system-meter unitary transition U in the space $\mathcal{H} \otimes \mathcal{H}_M$ [14, 16, 17],

$$K(a) = \langle a | U | \Omega \rangle \quad (13)$$

with the meter states $|\Omega\rangle$ and $|a\rangle$, assuming the meter initially in pure $|\Omega\rangle$ state, and measuring projectively $P_a = |a\rangle\langle a|$, calibrated to zero average bias for null detection,

$$\langle a \rangle_\Omega = \int da |\langle a | \Omega \rangle|^2 = 0. \quad (14)$$

The weak measurement can be defined by weakening $U \rightarrow U^\lambda$, with $\lambda \rightarrow 0$. It needs operational feasibility of the power which is realized for either $U \sim 1$ (already small disturbance) or continuous time evolution, e.g. $U = \exp(-i\lambda H)$. Then the evolution takes

$$\rho \rightarrow \lambda[H, \rho]/i \quad (15)$$

with the anticommutator notation $[A, B] \equiv AB - BA$, for $U = \exp(H/i)$ and Hermitian Hamiltonian H . After the measurement on the meter, one is left with the generic form [37–39, 50, 51],

$$\mathcal{K}\rho = \int da a K(a) \rho K^\dagger(a) \rightarrow \lambda(\{A, \rho\}/2 + i[B, \rho]) \quad (16)$$

with some operators F and G , and the anticommutator notation $\{F, G\} \equiv FG + GF$. The above remains true even if one adds some randomness of U and an additional λ -independent local transformation on the meter. For the Hamiltonian representation (15) we get

$$A/2 + iB = \int da \langle a | H | \Omega \rangle \langle \Omega | a \rangle / i. \quad (17)$$

Then $\langle a \rangle \rightarrow \lambda \langle A \rangle$ which makes B inaccessible in a single average. However, its effect can be captured by the next measurement or postselection. The part B is rather the influence of the detector on the system, which can occur also classically. In fact, classical indirect measurements have similar features as the quantum ones [39], except that they can be completely noninvasive. This is why we shall assume $B = 0$, although some measurement schemes (e.g. to measure emission noise [50, 51]) contain a special form of B .

From now on, we shall use the weak measurement superoperator

$$\mathcal{A} = \{A, \cdot\}/2, \quad (18)$$

assuming the known weak measurement protocol with some small λ as a scaling factor between the detector's outcome a and the observable A . In the case of symmetric dichotomic observables and projective measurements $A = \bar{a}(P_+ + P_-)$ with $K(\pm\bar{a}) = P_\pm$, the weak and projective measurements coincide as regards correlations, i.e.

$$\mathcal{A}\rho = \sum_a a K(a) \rho K^\dagger(a). \quad (19)$$

However, equation 19 is highly misleading, as the disturbance is very large and can be detected with measurement uncorrelated with a .

III. LG INEQUALITIES AND TIME ORDER

Suppose we have a single system and three observables, A, B, C with at least one of them measured non-invasively, see Fig. 2. Then, assuming the mapping of the measurement outcomes, $A \rightarrow a, B \rightarrow b, C \rightarrow c$, the correlations $\langle a \rangle, \langle ab \rangle$, or $\langle abc \rangle$ reflect the properties of some underlying probability distribution $p(a, b, c)$. If $|a|, |b| \leq 1$ then the LG inequality holds

$$\langle a \rangle + \langle b \rangle - \langle ab \rangle \leq 1. \quad (20)$$

It is valid both in classical and quantum mechanics, when applying direct sequence of measurement with outcomes

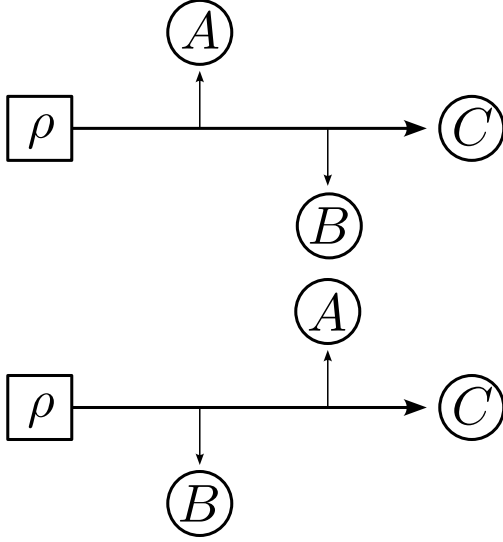


FIG. 2. The detection scheme to test LG inequalities and weak order of measurements. Two weak detectors of A and B measure the state ρ before the final measurement C . The time order of the measurement is from the left to the right: $A \rightarrow B \rightarrow C$ in the upper and $B \rightarrow A \rightarrow C$ in the lower case.

a and b . In general, measuring two outcomes is invasive. The problem arises when one demands reduction of invasiveness, which is only possible in the limit of weak measurements. However, by our theorem, we know the invasiveness is connected to the smaller sensitivity and indirect interpretation of the measurement results a and b . Suppose that we measure $A \rightarrow B$ (i.e. first A then B) weakly (replace $a \rightarrow \mathcal{A}$, $b \rightarrow \mathcal{B}$). As we work now with superoperators, let us define the averages, $\langle \mathcal{O} \rangle \equiv \text{Tr} \rho \mathcal{O} \mathbb{1}$ with the superoperator \mathcal{O} acting on identity $\mathbb{1}$. For the order $A \rightarrow B \rightarrow C$, where we measure weakly, we have $\langle \mathcal{ABC} \rangle = \text{Tr} \rho \mathcal{ABC} \mathbb{1}$, i.e. left to right time order.

Now the LG inequalities read

$$\begin{aligned} \langle \mathcal{A} \rangle + \langle \mathcal{B} \rangle - \langle \mathcal{AB} \rangle &\leq 1 \\ \langle \mathcal{A} \rangle + \langle \mathcal{B} \rangle - \langle \mathcal{BA} \rangle &\leq 1 \end{aligned} \quad (21)$$

measuring $A \rightarrow B$ and $B \rightarrow A$, respectively. Moreover, classical noninvasive measurements cannot depend on their order,

$$\langle \mathcal{ABC} \rangle = \langle \mathcal{BAC} \rangle \quad (22)$$

with the first order $A \rightarrow B \rightarrow C$ and the second order $B \rightarrow A \rightarrow C$. In contrast, quantum correlations, even noninvasive, depend on the order,

$$\langle \mathcal{ABC} \rangle - \langle \mathcal{BAC} \rangle = \langle [[A, B], C] \rangle / 4. \quad (23)$$

In our approach we shall (i) assume that all three observables are dichotomic $A^2 = B^2 = C^2 = 1$, (ii) the measurement scheme is also dichotomic, as described by (11) with $A, B \rightarrow \lambda A, \lambda B$ measured weakly, and C projectively (formally $\lambda_C = 1$). The exact formulas for all correlations in this schemes are given in Appendix B.

$$a \begin{array}{|c|} \hline \downarrow \\ \hline \end{array} b = \begin{array}{|c|} \hline \begin{array}{|c|} \hline CR^+ \\ \hline \end{array} \begin{array}{|c|} \hline X \\ \hline \end{array} \begin{array}{|c|} \hline CR^- \\ \hline \end{array} \\ \hline \end{array}$$

FIG. 3. The notation of the ECR gate in the convention $ECR_{\downarrow}|ab\rangle$.

$$\boxed{Z_{\theta}} = |0\rangle \begin{array}{|c|} \hline \begin{array}{|c|} \hline X_+ \\ \hline \end{array} \begin{array}{|c|} \hline Z_+ \\ \hline \end{array} \begin{array}{|c|} \hline Z_{\theta} \\ \hline \end{array} \begin{array}{|c|} \hline X_+ \\ \hline \end{array} \begin{array}{|c|} \hline \bullet \\ \hline \end{array} \begin{array}{|c|} \hline \oplus \\ \hline \end{array} \begin{array}{|c|} \hline \text{meter} \\ \hline \end{array} \\ \hline \end{array}$$

FIG. 4. Protocol (I) with a single CX gate. Weak measurement of Z on the upper qubit, by the lower (meter) qubit with the strength of the measurement defined by $\sin \theta$. The control and target qubit are depicted by \bullet and \oplus respectively.

We set initial state $\rho = |\psi\rangle\langle\psi|$ with $\sqrt{2}|\psi\rangle = |+\rangle + |-\rangle$, and the observables

$$\begin{aligned} A &= e^{i\pi/4}|+\rangle\langle-| + e^{-i\pi/4}|-\rangle\langle+| \\ B &= e^{-i\pi/4}|+\rangle\langle-| + e^{i\pi/4}|-\rangle\langle+| \\ C &= i|-\rangle\langle+| - i|+\rangle\langle-| \end{aligned} \quad (24)$$

Then

$$\begin{aligned} \langle \mathcal{A} \rangle &= \langle \mathcal{B} \rangle = 1/\sqrt{2} \\ \langle \mathcal{AB} \rangle &= \langle \mathcal{BA} \rangle = 0, \\ \langle \mathcal{ABC} \rangle &= -\langle \mathcal{BAC} \rangle = 1/2 \end{aligned} \quad (25)$$

which violates (21) as $\sqrt{2} > 1$ and (22) as $1/2 \neq -1/2$.

IV. WEAK MEASUREMENTS ON IBM AND IONQ

IBM Quantum offers networks of qubits, i.e. local two-level spaces, with the default basis $|0\rangle, |1\rangle$. The states can be changed by unitary operations (gates). The qubit is usually measured projectively in the default basis, as the states differ by energy and lose mutual coherence over time. However, all projections are feasible, by the use of quantum gates. To realize weak measurement on a qubit, it must be entangled with an auxiliary meter qubit by a two-qubit operation/gate. We have implemented two different protocols of weak measurement:

- (I) the meter is close to the special state $\sim |\Omega\rangle$ for which applying the operation V' does not affect

$$\boxed{Z_{\theta}} = |0\rangle \begin{array}{|c|} \hline \begin{array}{|c|} \hline X_{\theta} \\ \hline \end{array} \begin{array}{|c|} \hline \bullet \\ \hline \end{array} \begin{array}{|c|} \hline Z \\ \hline \end{array} \begin{array}{|c|} \hline X_+ \\ \hline \end{array} \begin{array}{|c|} \hline \text{meter} \\ \hline \end{array} \\ \hline \end{array}$$

FIG. 5. Protocol (I) with a single CZ gate and a fractional RX , represented by X_{θ} . Weak measurement of Z on the upper qubit, by the lower (meter) qubit with the strength of the measurement defined by $\sin \theta$. The CZ gate is depicted as linked \bullet (the gate is symmetric).

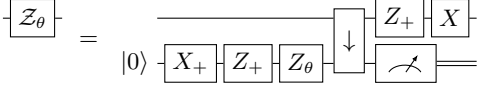


FIG. 6. Protocol (I), with a single *ECR* gate. Weak measurement of Z on the upper qubit, by the lower (meter) qubit with the strength of the measurement defined by $\sin \theta$.

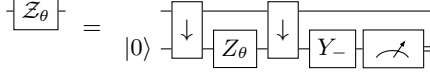


FIG. 7. Protocol (II), with two *ECR* gates. Weak measurement of Z on the upper qubit, by the lower (meter) qubit with the strength of the measurement defined by $\sin \theta$.

the system, i.e. $V'|\psi\rangle|\Omega\rangle = |\psi\rangle|\Omega\rangle$ for an arbitrary $|\psi\rangle$ [52–54],

(II) the constructed operation U is ~ 1 , i.e. close to identity [46].

The protocol (I) involves a single entangling operation. Its small invasiveness relies on a specifically prepared meter state. On the other hand (II) technically needs either two self-reverse entangling operations or a single true incremental operation which is noninvasive regardless of the meter state. Therefore (II) is closer to the universal derivation of weak measurements from weak entanglement. Nevertheless, both protocols result in the same POVM and their implementation on IBM is feasible. To apply (I), we can restrict V' to a unitary V in the subspace orthogonal to $|\Omega\rangle$. One prepares the state close to $|\Omega\rangle$,

$$|\Omega_\theta\rangle = |\Omega_\perp\rangle \sin \theta/2 + |\Omega\rangle \cos \theta/2, \quad (26)$$

where $\langle \Omega_\perp | \Omega \rangle = 0$. Note that $\langle \Omega | V | \Omega_\perp \rangle = 0$ by unitarity, so the invasiveness is $\sim \theta^2$. We construct Kraus operators analogously to (13),

$$K(a) = \langle a | U | \Omega_\perp \rangle \sin \theta/2 + \langle a | \Omega \rangle \cos \theta/2. \quad (27)$$

Assuming unbiased measurement by (14) and $\lambda = \sin \theta$ we get the weak limits (16),

$$A + 2iB = \int da a \langle \Omega | a \rangle \langle a | U | \Omega_\perp \rangle. \quad (28)$$

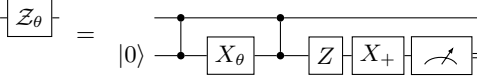


FIG. 8. Protocol (II), with two *CZ* gates and fractional *RX* gate, represented by X_θ . Weak measurement of Z on the upper qubit, by the lower (meter) qubit with the strength of the measurement defined by $\sin \theta$.

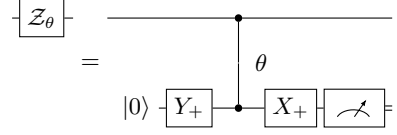


FIG. 9. Protocol (II), with a single $(ZZ)_\theta$ gate. Weak measurement of Z on the upper qubit, by the lower (meter) qubit with the strength of the measurement defined by $\sin \theta$. $(ZZ)_\theta$ gate is depicted as a link between the qubits.

In the case of purely dichotomic measurement with $a = \pm 1$ (shortly \pm) and $V^2 = \mathbb{1}$ (parity operation) we can set

$$\begin{aligned} \sqrt{2}|\Omega\rangle &= |+\rangle + |-\rangle, \\ \sqrt{2}|\Omega_\perp\rangle &= |+\rangle - |-\rangle, \end{aligned} \quad (29)$$

to obtain (11) for $A = \lambda V$.

The protocol (II) also simplifies for dichotomic measurement taking $U_\theta = \exp(-iVW\theta/2)$ with V acting in the system space and W acting in the meter space, such that $V^2 = W^2 = \mathbb{1}$, $V = V^\dagger$, $W = W^\dagger$. We construct the states (29) with $W|\Omega\rangle = i|\Omega_\perp\rangle$ i.e. W reads in the basis $|+\rangle, |-\rangle$

$$\begin{pmatrix} 0 & i \\ -i & 0 \end{pmatrix}. \quad (30)$$

Then again we obtain (11) for $A = \lambda V$.

V. IMPLEMENTATION ON IBM

For the physical implementation and manipulation of qubits as transmons [55] and programming of IBM Quantum, see [56–58]. To describe the actual implementation of the test from Sec. III, we start from Pauli matrices in the basis $|+\rangle \equiv |0\rangle$, $|-\rangle \equiv |1\rangle$. This is the natural convention in quantum computing, switching between spin and bit notation. The explicit form of Pauli matrices is

$$X = \begin{pmatrix} 0 & 1 \\ 1 & 0 \end{pmatrix}, Y = \begin{pmatrix} 0 & -i \\ i & 0 \end{pmatrix}, Z = \begin{pmatrix} 1 & 0 \\ 0 & -1 \end{pmatrix}, I = \begin{pmatrix} 1 & 0 \\ 0 & 1 \end{pmatrix}. \quad (31)$$

Now, the $|\pm\rangle$ are eigenstates of $Z|\pm\rangle = \pm|\pm\rangle$. The IBM Quantum devices use transmon qubits. Such systems natively support X gate and

$$X_+ = X_{\pi/2} = (I - iX)/\sqrt{2} = \begin{pmatrix} 1 & -i \\ -i & 1 \end{pmatrix}/\sqrt{2}, \quad (32)$$

denoting $V_\theta = \exp(-i\theta V/2) = \cos(\theta/2) - iV \sin(\theta/2)$. Furthermore, we also denote $V_\pm = V_{\pm\pi/2}$, whenever V^2 is identity. Note that $Z_\theta = \exp(-i\theta Z/2) = \text{diag}(e^{-i\theta/2}, e^{i\theta/2})$ is a virtual gate, essentially adding the phase shift to next gates. A sequence of these operations allows one to realize an arbitrary unitary gate U . The standard projective measurement is implemented by $P_a = |a\rangle\langle a|$ for $a = 0, 1$. One can also see that

G	C	A	B	$eCA[10^{-2}]$	$eCB[10^{-2}]$	$eC[10^{-2}]$	$eA[10^{-2}]$	$eB[10^{-2}]$
brisbane								
0	94	95	90	1.4	0.86	1.7	2.9	0.93
1	6	5	7	0.62	0.53	1.2	1	2.1
2	58	71	59	0.36	0.41	1.3	1.2	1.9
3	62	61	63	0.63	0.66	1.4	1.1	1.1
4	52	37	56	0.58	0.8	1.3	0.9	2.3
5	116	115	117	1.1	0.58	2.2	1.9	1.9
6	50	49	51	1.4	1.3	2.8	0.95	3.7
7	21	20	22	0.66	0.41	0.88	2.3	2.2
8	125	124	126	0.68	0.79	1.4	1.4	1.6
9	108	112	107	0.66	0.79	1.2	0.85	2.1
sherbrooke								
0	49	50	48	0.39	1.2	5.4	3	1.6
1	107	106	108	0.77	0.74	3	1.3	0.88
2	119	118	120	0.67	0.76	0.78	0.9	1.1
3	45	46	44	0.65	0.67	1.4	5.1	0.71
4	69	68	70	0.46	0.49	2.4	1.1	17
5	59	60	58	1.1	1	1.9	1.2	1.1
6	89	88	74	1.1	0.82	5.4	3.7	1.2
7	114	109	115	0.45	1.6	1.5	2.8	7.2
8	26	25	27	0.93	0.68	0.9	2.5	0.9
9	80	79	81	0.83	0.62	0.83	1.2	0.59
kyiv								
0	53	60	41	0.34	0.34	0.88	0.63	0.34
1	114	115	113	1.2	1.8	1.5	0.51	3
2	0	1	14	0.41	0.53	0.73	1.2	1.3
3	68	69	55	0.76	0.63	1.2	0.27	2.8
4	26	16	25	1	1.1	2.1	3.2	1.4
5	4	3	15	1	1.1	8.2	0.54	2
6	103	102	104	0.48	1	0.42	2.2	1
7	82	83	81	0.59	1.3	0.56	1.5	2.2
8	54	45	64	0.96	1.2	0.71	0.37	0.71
9	33	20	39	0.64	1.6	0.39	5.4	1.6

TABLE I. Devices from Eagle generation, groups (G) with measured qubits, main (system) C , auxiliary (meters) A and B , errors of ECR/ZZ gates between qubit C and A/B , and readout errors on qubits C , A , B .

$Z = P_0 - P_1$ represents the outcome $z = \pm 1$. The measurement can be done along any axis by using a unitary rotation $M = U^\dagger Z U$.

To measure weakly, we have to couple the system qubit with an auxiliary meter. We shall describe two-qubit gates using the following, shorthand notation $(AB)|ab\rangle = (A|a\rangle)(B|b\rangle)$. The commonly used gate is controlled rotation, CU , e.g. CX (also known as $CNOT$) or CZ . Matrix form of CU gate, in the $\{|00\rangle, |01\rangle, |10\rangle, |11\rangle\}$ basis is

$$\begin{pmatrix} I & 0 \\ 0 & U \end{pmatrix} \quad (33)$$

or equivalently

$$CU = (II + ZI + IU - ZU)/2. \quad (34)$$

For $CU|ab\rangle$ the control qubit is a and the target is b and U is applied to $|b\rangle$ only if $a = 1$. By local rotation V on qubit b one can freely change $U \rightarrow V^\dagger U V$. In the protocol (I), the states $|\Omega\rangle$ and $|\Omega_\perp\rangle$ should be the

eigenstates of U . For $U = X$ we have

$$\begin{aligned} |\Omega\rangle &= (|0\rangle + |1\rangle)/\sqrt{2} \\ |\Omega_\perp\rangle &= (|0\rangle - |1\rangle)/\sqrt{2}. \end{aligned} \quad (35)$$

Protocol (I) is realized in the following way. We take

$$\begin{aligned} |\Omega_\theta\rangle &= X_+ Z_{\theta+\pi/2} X_+ |0\rangle = \\ &= \sin(\theta/2 + \pi/4) |0\rangle + \cos(\theta/2 + \pi/4) |1\rangle, \end{aligned} \quad (36)$$

apply $CX|\psi\Omega_\lambda\rangle$, assuming system state $|\psi\rangle$ and measure $Z \rightarrow \pm 1$ on the meter qubit. One can notice that we end up with the scheme (11) for $A = \lambda Z$ with $\lambda = \sin \theta$, Fig. 4, i.e.

$$\sqrt{2}K_\pm = \cos \theta/2 + Z \sin \theta/2. \quad (37)$$

Instead of CX , the native gate on IBM Heron devices, like `ibm_torino`, is CZ [59], and one can use a new single-qubit fractional $RX(\theta) \equiv X_\theta$. This enforces a slight modification of protocol (I) implementation. The prepared

G	C	A	B	$CZeCA[10^{-2}]$	$RZZeCA[10^{-2}]$	$CZeCB[10^{-2}]$	$RZZeCB[10^{-2}]$	$eC[10^{-2}]$	$eA[10^{-2}]$	$eB[10^{-2}]$
torino										
0	88	87	94	0.31	1.3	0.3	0.62	5.9	0.9	0.98
1	29	28	36	0.33	0.62	0.22	0.39	1.5	0.85	0.56
2	12	13	18	0.24	0.22	0.37	0.15	2.2	0.71	0.49
3	46	47	55	0.34	0.77	0.23	0.31	4.5	1.3	0.63
4	61	54	60	0.37	0.66	0.22	0.44	1.5	0.68	1.1
5	33	32	37	0.3	1.3	0.28	0.26	1.3	2	0.42
6	10	9	11	0.25	0.49	0.32	0.3	2.5	1.9	0.93
7	80	81	92	0.25	0.45	0.15	0.3	1.6	0.81	0.39
8	50	49	51	0.31	0.29	0.37	0.35	9.3	1.7	1.5
9	44	35	43	0.2	0.41	0.23	0.4	1.9	1.6	0.88
kingston										
0	129	118	128	0.12	0.14	0.17	0.085	2	0.2	0.56
1	83	82	96	0.21	0.16	0.19	0.15	0.56	0.42	0.39
2	141	140	142	0.15	0.14	0.14	0.16	0.49	0.63	0.61
3	104	103	105	0.2	0.32	0.14	0.19	0.34	1.3	0.51
4	125	117	126	0.24	0.55	0.3	0.2	7.6	0.34	0.46
5	49	38	50	0.17	0.13	0.24	0.41	0.49	0.88	0.71
6	14	13	15	0.14	0.3	0.6	0.18	2.4	1.1	0.63
7	63	62	64	0.17	0.39	0.21	0.45	0.85	1.1	0.37
8	70	69	71	0.22	0.41	0.26	0.34	1.9	0.59	0.44
9	67	57	68	0.43	0.37	0.15	0.19	0.81	0.44	0.54

TABLE II. Devices from Heron generation, groups (G) with measured qubits, main (system) C , auxiliary (meters) A and B , errors of CZ/RZZ gates between qubit C and A/B , and readout errors on qubits C , A , B .

meter state is

$$|\Omega_\theta\rangle = X_\theta |0\rangle = \cos(\theta/2) |0\rangle - i \sin(\theta/2) |1\rangle \quad (38)$$

instead, and one measures $-Y$, see Fig. 5.

The IBM Quantum devices use a native asymmetric two-qubit ECR gates instead of CX , but one can transpile the latter with the former, by adding single-qubit gates. The ECR gate acts on the states $|ab\rangle$ as (Fig. 3)

$$ECR_\downarrow = ((XI) - (YX))/\sqrt{2} = CR^-(XI)CR^+ =$$

$$\begin{pmatrix} 0 & X_- \\ X_+ & 0 \end{pmatrix} = \begin{pmatrix} 0 & 0 & 1 & i \\ 0 & 0 & i & 1 \\ 1 & -i & 0 & 0 \\ -i & 1 & 0 & 0 \end{pmatrix} / \sqrt{2}, \quad (39)$$

in the basis $|00\rangle, |01\rangle, |10\rangle, |11\rangle$, with Crossed Resonance gates

$$CR^\pm = (ZX)_{\pm\pi/4}. \quad (40)$$

The gate is its inverse, i.e. $ECR_\downarrow ECR_\downarrow = (II)$. The protocol (I) can be still realized by $CX = (XI)(Z_+I)ECR_\downarrow(IX_-)$, see Fig. 6. The protocol (II) needs an operation ~ 1 which is realized by two ECR gates with a small phase shift on the meter (target) qubit

$$(ZY)_\theta = II \cos(\theta/2) - iZY \sin(\theta/2)$$

$$ECR_\downarrow(IZ_\theta)ECR_\downarrow \quad (41)$$

on IBM Eagle. The meter qubit is initially in the state $|0\rangle$ and finally measured by $X = \pm 1$. It is possible by applying Y_- rotation before readout since $Y_+ZY_- = -iYZ =$

X , see Fig. 7. In the case of IBM Heron devices, one uses two CZ gates and again a fractional $RX(\theta)$ gate, followed by measuring $-Y$, see Fig. 8. The resulting POVM is identical to the protocol (I). Both protocols measure any unit combination of Pauli matrices by appropriate unitary transform $Z \rightarrow U^\dagger Z U$, with U and U^\dagger applied before and after the protocol, respectively.

Importantly, the protocol (II) on Heron and IonQ uses native symmetric fractional gates $(ZZ)_\theta$,

$$\begin{pmatrix} e^{i\theta/2} & 0 & 0 & 0 \\ 0 & e^{-i\theta/2} & 0 & 0 \\ 0 & 0 & e^{-i\theta/2} & 0 \\ 0 & 0 & 0 & e^{i\theta/2} \end{pmatrix} \quad (42)$$

with the initial detector's state $(|0\rangle - i|1\rangle)/\sqrt{2} = X_+|0\rangle$ and measuring along X basis by applying Y_- before the measurement. Since IBM allows only $\theta > 0$, we reversed the sign by $Y_+ \rightarrow Y_-$, see Fig. 9. One can find further details about the circuits we used in Appendix C.

VI. RESULTS

We have tested 10 sets of 3 qubits on 3 IBM Eagle devices: `ibm_brisbane`, `ibm_sherbrooke`, `ibm_kyiv`, and 2 IBM Heron devices `ibm_torino` and `ibm_kingston`, see details in Tables I, II. We ran 60/40 jobs on Eagle/Heron, each one with 10000 shots, 25 repetitions of $A \rightarrow B \rightarrow C$ and $B \rightarrow A \rightarrow C$ measurement orders for $\theta = \pm 0.1$ (i.e. 2×2 measurements). The actual measurement is

the projection on the states $|abc\rangle$ where a, b are the outcomes of auxiliary meter qubits, corresponding to weak measurement of A and B , respectively, while c is the final projection on the system qubit. To eliminate drifts, we have taken the difference of results for $\theta = \pm 0.1$ and divided the difference by $2\lambda = 2\sin|\theta|$. It gives a total of 8 circuits per measurement scheme, with $25 \times 8 = 200$ circuits in each job, randomly shuffled to avoid memory-related effects.

The results of Leggett-Garg test on observables A and B , are shown in Fig. 10 while the test of time order is presented in Fig. 11. We denoted weak measurement performed by protocols (I) and (II) by $1ECR/CZ$ and $2ECR/CZ$, respectively. To calculate the error, we assumed that shots are identical and independent of each other. This allowed us to use the Bernoulli formula in our analysis. For weak measurements, \mathcal{A} and \mathcal{B} , the actual product of values ab is almost uniform with random values ± 1 . This makes the almost identical error of each of correlations Q of the form $\langle \mathcal{AB} \rangle$ or $\langle \mathcal{ABC} \rangle$ and $\mathcal{A} \leftrightarrow \mathcal{B}$. It is just scaled by the assumed measurement strength. We add up all 4 strength combinations to get the final error scaled by the total number of experiments,

$$\sqrt{\langle (Q - \langle Q \rangle)^2 \rangle} \simeq 1/2\sqrt{JSR}\sin^2(\theta) \quad (43)$$

for J jobs S shots and R repetitions, here $\simeq 0.013$. It is much smaller than the observed violations.

In the case of LG, we summed up errors treating correlations as independent of single average $\langle \mathcal{A} \rangle$ and $\langle \mathcal{B} \rangle$, but the correlation contribution dominates at least $1/\lambda$ times. There is also a small correction by invasiveness, of the order λ^2 , which is negligible in this case, see Appendix D. The LG violation is about 10 standard deviations, except for isolated sets of qubits. The same applies to the time order violation. Note that the third order correlation is identical when applying a sequence of 3 projective measurements, but then the invasiveness is obvious.

The results were different on the `ibm_torino` and `ibm_kingston`, with fractional $(ZZ)_\theta$ gate. We collected the data using the same θ but with Y_\pm in the weak measurement circuit, see Fig. 9. This way we were able to get the measurement strength parametrized by $\pm\theta$. LG inequality was violated only for qubit group 4 on `ibm_torino` but at least 5 groups on `ibm_kingston`, see Fig. 12. However, all the groups passed the test of time order, see 13. Surprisingly, only the difference between correlations for ABC and BAC orders remains roughly stable, while individual correlations vary across qubit groups.

We have also tested IonQ, Forte Enterprise 1, on a single set of 3 qubits. Formally those were 0,1,2, but ion trap technology makes them all equivalent. In those experiments we ran 2 jobs, 100000 shots and 25 repetitions each. The circuit was formally identical to the one ran on `ibm_torino` and `ibm_kingston`. The tested device contains 36 ions $^{171}\text{Yb}^+$, with the drive frequency 12.64GHz between hyperfine levels, in a linear Paul trap with expected average 1 and 2-qubit gate errors 0.08%

and 5.14%, respectively. For technical details see the documentation [62–68].

The results, presented in Table III, show violation of LG inequality and order dependence, even exceeding quantum expectations. The origin of that phenomenon could be a miscalibration of $(ZZ)_\theta$ gate for the angle θ passed to the device. A deviation by about 5% from the actual θ , i.e. of the order of 2-qubit gate error, would explain the excess results. Due to longer gate times and repetition rates, the whole test took about two months, comparing to several hours on IBM.

All correlations and averages are presented in Appendix E. The data and the scripts we used are available publicly [69].

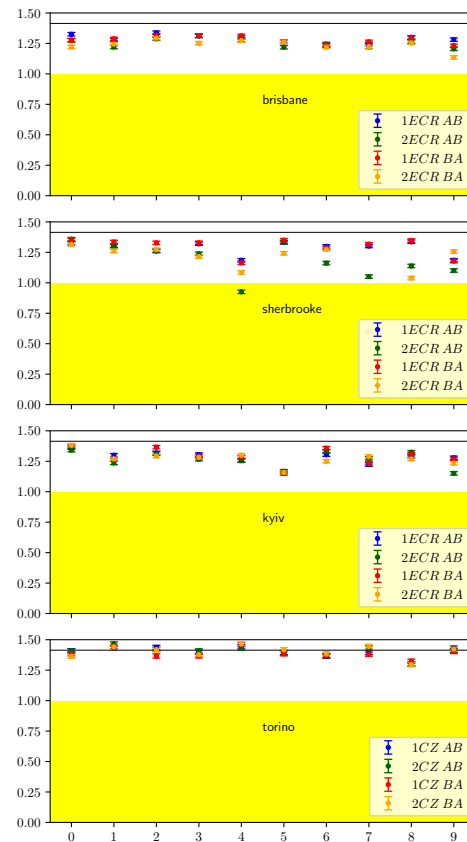


FIG. 10. Leggett-Garg violation for qubits from the tested IBM devices (see Tables I,II). The values correspond to the combination of correlations taken from Eq. (C4). The results $nECR/CZ$ correspond to $n = 1, 2$ gates ECR/CZ , while AB and BA correspond to the order $A \rightarrow B$ and $B \rightarrow A$. The solid line is the perfect value $\sqrt{2}$ while the yellow region is below the classical limit.

VII. DISCUSSION

We have shown that weak measurements can be realized on IBM Quantum and similar public quantum computers to demonstrate incompatibility between noninva-

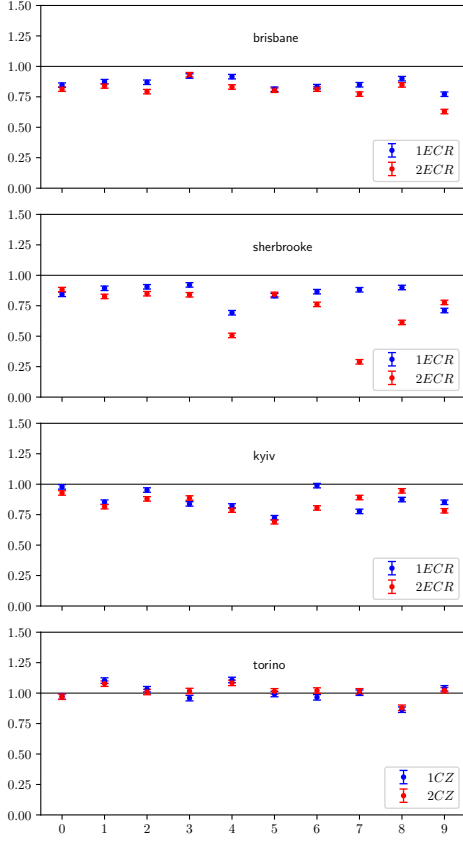


FIG. 11. Order invariance violation for qubits from the tested IBM devices (see Tables I, II). The values correspond to the difference $\langle ABC \rangle - \langle BAC \rangle$. The results $nECR/CZ$ correspond to $n = 1, 2$ gates ECR/CZ . The solid line is the perfect value 1.

siveness and realism, by means of LG and time order violation. In the case of LG, we had to assume the strength of the measurement, so further improvements on LG test are needed in this respect. Both violations are significant. One can have an objection that the gates are strong and invasive, even in the case of self-reversal. It might be possible to replace the native ECR gate by its customized (via pulse modification) version, reducing the interaction strength. The newly introduced fractional single-qubit RX gate works excellent on IBM Heron devices, however its two-qubit relative, RZZ , works significantly worse. The question of whether the strength of fractional gates is accurately reduced remains ambiguous. On one hand, the time order violation is clear, on the other hand, the LG inequality is randomly violated. It seems that IonQ Forte and `ibm_kingston` are ahead, proving the technological progress in both implementations. Nevertheless, large deviations from theoretical expectations, despite small declared error, need urgent explanation. Another open question concerns usefulness of weak measurements in quantum computation. Although the price for the small invasiveness is the necessity of large statistics, the actual trade-off is yet to be evaluated.

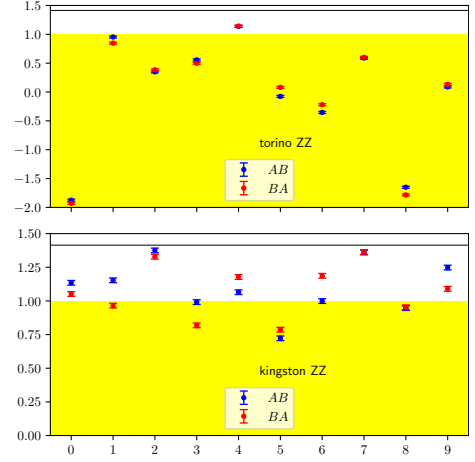


FIG. 12. Leggett-Garg violation for fractional RZZ gate devices (`ibm_torino` and `ibm_kingston`) for each qubits set (see Table II). The values correspond to the combination of correlations taken from Eq. (C4), while AB and BA correspond to the order $A \rightarrow B$ and $B \rightarrow A$. The solid line is the perfect value $\sqrt{2}$ while the yellow region is below the classical limit.

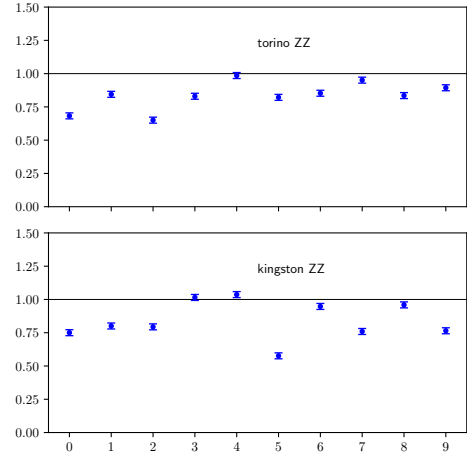


FIG. 13. Order invariance violation for fractional RZZ gate devices (`ibm_torino` and `ibm_kingston`) for each qubits set (see Table II). The values correspond to the difference $\langle ABC \rangle - \langle BAC \rangle$. The solid line is the perfect value 1.

ACKNOWLEDGMENTS

The results have been created using IBM Quantum. The views expressed are those of the authors and do not reflect the official policy or position of the IBM Quantum team. TR gratefully acknowledges the funding support by program "Excellence initiative – research university" for the AGH University in Krakow as well as the ARTIQ project: UMO-2021/01/2/ST6/00004 and ARTIQ/0004/2021. We thank Poznań Supercomputing and Networking Center and ICM UW for the access to IBM Quantum Innovation Center.

quantity	value	error
LGAB	1.583	0.025
LGBA	1.569	0.025
order	1.190	0.032
$\langle ABC \rangle$	0.630	0.022
$\langle BAC \rangle$	-0.560	0.022
$\langle AB \rangle$	0.020	0.022
$\langle BA \rangle$	0.004	0.022
$\langle AbC \rangle$	-0.768	0.002
$\langle bAC \rangle$	-0.786	0.002
$\langle aBC \rangle$	0.790	0.002
$\langle BaC \rangle$	0.783	0.002
$\langle Ab \rangle$	0.799	0.002
$\langle bA \rangle$	0.787	0.002
$\langle aB \rangle$	0.790	0.002
$\langle Ba \rangle$	0.800	0.002
$\langle abC \rangle$	0.011	0.0002
$\langle baC \rangle$	0.008	0.0002

TABLE III. The values and errors from the test on IonQ. Here LGAB and LGBA refer to LG inequalities Eq. (C4) for the order $A \rightarrow B$ and $B \rightarrow A$, and order = $\langle ABC \rangle - \langle BAC \rangle$. The remaining correlations and averages follow the rule: capital letter A, B – outcome matters, small letter a, b outcome ignored. The order of letters corresponds to the order of measurements. For instance $\langle AbC \rangle$ means correlation between A and C with the weak measurement of B , which occurred after A , but was ignored.

Appendix A: Proof of the Theorem 1

By convexity we can assume that $\rho_{\pm} = |\pm_0\rangle\langle\pm_0|$ for some orthogonal states $|\pm_0\rangle$. Let us assume $\langle a \rangle_{\pm} = \pm\Delta/2$ by shifting $a \rightarrow a - (\langle a \rangle_+ + \langle a \rangle_-)/2$. We define two states, being the superpositions of $|\pm_0\rangle$, i.e.

$$\sqrt{2}|\pm\rangle = |+_0\rangle \pm |-_0\rangle. \quad (\text{A1})$$

Then

$$\begin{aligned} \Delta &= \int da a \text{Tr} K^\dagger(a) K(a) (|+_0\rangle\langle+_0| - |-_0\rangle\langle-_0|) \\ &= \int da a \text{Tr} K^\dagger(a) K(a) (|-\rangle\langle+| + |+\rangle\langle-|). \end{aligned} \quad (\text{A2})$$

We apply the Cauchy-Schwarz inequality $\langle v|v\rangle\langle w|w\rangle \geq |\langle v|w\rangle|^2$ to

$$\begin{aligned} |v\rangle &= aK(a)|\pm\rangle, \\ |w\rangle &= (P_{\mp} + P/2)K(a)|\mp\rangle \end{aligned} \quad (\text{A3})$$

for $P_{\pm} = |\pm\rangle\langle\pm|$ and $P = 1 - P_+ - P_-$ being the projectors onto three relevant subspaces. then

$$\langle w|w\rangle = \langle K^\dagger(a)(P_{\mp} + P/4)K(a)\rangle_{\mp} \quad (\text{A4})$$

and

$$\begin{aligned} \sum_{\pm} \int da \sqrt{\langle K^\dagger(a)a^2K(a)\rangle_{\pm} \langle K^\dagger(a)(P_{\pm} + P/4)K(a)\rangle_{\mp}} \\ \geq \Delta/2 \end{aligned} \quad (\text{A5})$$

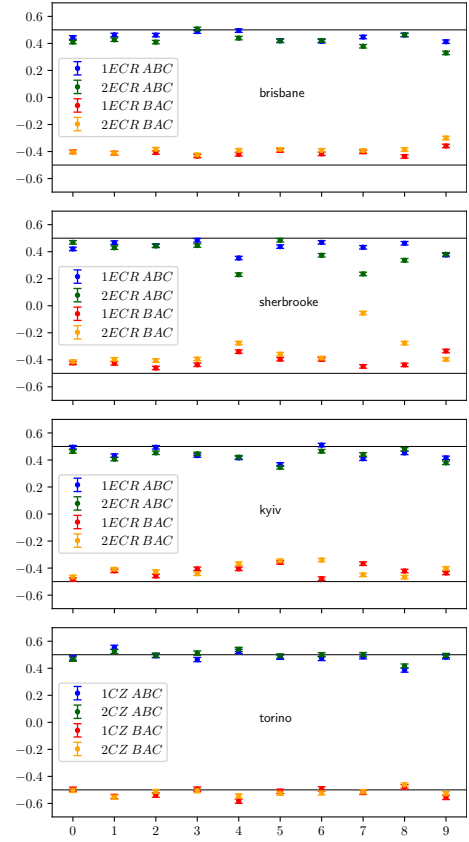


FIG. 14. Correlations $\langle ABC \rangle$ and $\langle BAC \rangle$ on the respective IBM devices. Description $nECR/CZ$ corresponds to $n = 1, 2$ ECR/CZ gate(s) in the protocol, while ABC and BAC correspond to the order $A \rightarrow B$ and $B \rightarrow A$. The solid lines are the perfect values ± 0.5 .

with the subscript \pm for the states $\rho = P_{\pm}$. We can replace $P/4$ by P not decreasing the left hand side. By the Cauchy-Schwarz inequality

$$\left(\int f g da \right)^2 \leq \int f^2 da \int g^2 da \quad (\text{A6})$$

applied to

$$\begin{aligned} f^2 &= \langle K^\dagger(a)a^2K(a)\rangle_{\pm}, \\ g^2 &= \langle K^\dagger(a)(P_{\pm} + P)K(a)\rangle_{\mp} \end{aligned} \quad (\text{A7})$$

we get

$$\sum_{\pm} \sqrt{\langle a^2 \rangle_{\mp} \eta_{\pm}} \geq \Delta/2 \quad (\text{A8})$$

for

$$\eta_{\pm} = 1 - \int da |\langle K(a) \rangle_{\pm}|^2 \quad (\text{A9})$$

We chose $\rho = P_{\pm}$ with the larger value $\langle a^2 \rangle_{\mp} \eta_{\pm}$ and finally get

$$16\sigma^2 E \geq \Delta^2 \quad (\text{A10})$$

which completes the proof.

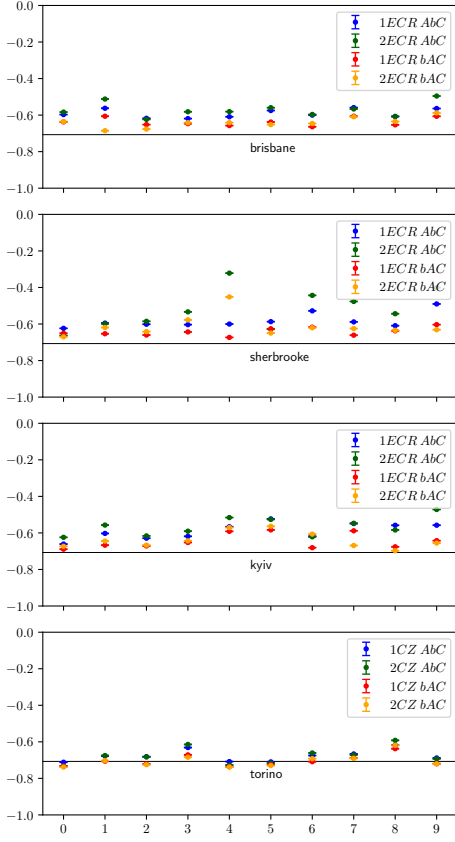


FIG. 15. Correlations $\langle \mathcal{AC} \rangle$ on the respective IBM devices. Description $nECR/CZ$ corresponds to $n = 1, 2$ ECR/CZ gate(s) in the protocol, while AbC and bAC correspond to the order $A \rightarrow B$ and $B \rightarrow A$. The solid line is the perfect value $-1/\sqrt{2}$.

Appendix B: Measurements of dichotomic observables with arbitrary strength

The full treatment of weak measurement of the strength λ requires two superoperators

$$\mathcal{A}\rho = \sum_a a K_\lambda(a) \rho K_\lambda^\dagger(a) / \lambda \quad (\text{B1})$$

with

$$K_\lambda(a) = \sqrt{(1 + \lambda a A)/2} \quad (\text{B2})$$

and $a = \pm 1$, i.e. outcomes of the measurement on the meter qubits, which reduces to

$$\sqrt{2} K_\lambda(a) = \cos(\theta/2) + A \sin(\theta/2) \quad (\text{B3})$$

and $\mathcal{A} = \{A, \cdot\}/2$ for $\lambda = \sin \theta$. If one ignores the measurement, there is still invasiveness

$$\tilde{\mathcal{A}}\rho = \sum_a K_\lambda(a) \rho K_\lambda^\dagger(a) \quad (\text{B4})$$

reducing to

$$\tilde{A} = 1 - g \mathcal{G}_A \quad (\text{B5})$$

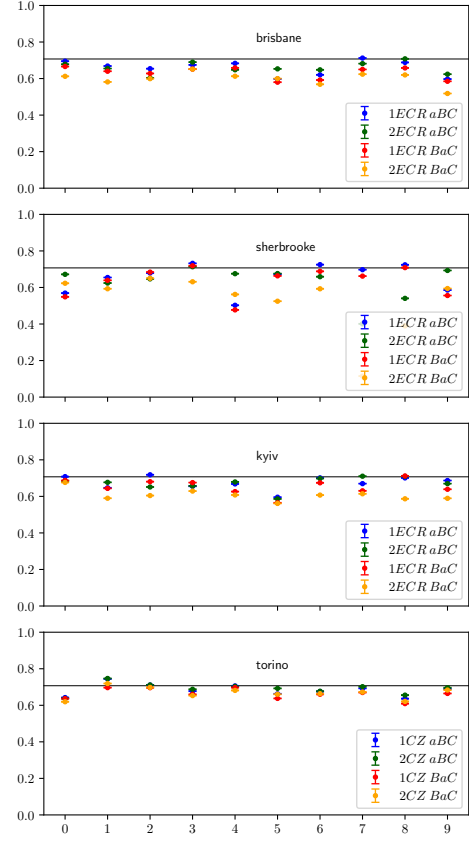


FIG. 16. Correlations $\langle \mathcal{BC} \rangle$ on the respective IBM devices. Description $nECR/CZ$ corresponds to $x = 1, 2$ ECR/CZ gate(s) in the protocol, while aBC and BaC correspond to the order $A \rightarrow B$ and $B \rightarrow A$. The solid lines are the perfect values $1/\sqrt{2}$.

with $\mathcal{G}_A = [A, [A, \cdot]]$ for dichotomic A and

$$g = \sin^2(\theta/2)/2 = (1 - \sqrt{1 - \lambda^2})/4 \sim \lambda^2/8 \quad (\text{B6})$$

In the eigenbasis $|+\rangle, |-\rangle$ of $A = |+\rangle\langle+| - |-\rangle\langle-|$, the superoperators read

$$\mathcal{A} \begin{pmatrix} \rho_{++} & \rho_{+-} \\ \rho_{-+} & \rho_{--} \end{pmatrix} = \begin{pmatrix} \rho_{++} & 0 \\ 0 & \rho_{--} \end{pmatrix} \quad (\text{B7})$$

while

$$\tilde{\mathcal{A}} \begin{pmatrix} \rho_{++} & \rho_{+-} \\ \rho_{-+} & \rho_{--} \end{pmatrix} = \begin{pmatrix} \rho_{++} & \rho_{+-} \cos \theta \\ \rho_{-+} \cos \theta & \rho_{--} \end{pmatrix}. \quad (\text{B8})$$

This POVM also captures projection at $\lambda = 1$, $\theta = \pi/2$ and $g = 1/4$.

Let all observables A, B, C , be dichotomic. Note that the strength of the last measurements is irrelevant. In the case of a single weak measurement of A followed by C the readout correlation is equal and the backaction corrected measurement read

$$\langle \tilde{\mathcal{A}}C \rangle = \langle C \rangle - \langle \mathcal{G}_A C \rangle g_A, \quad (\text{B9})$$

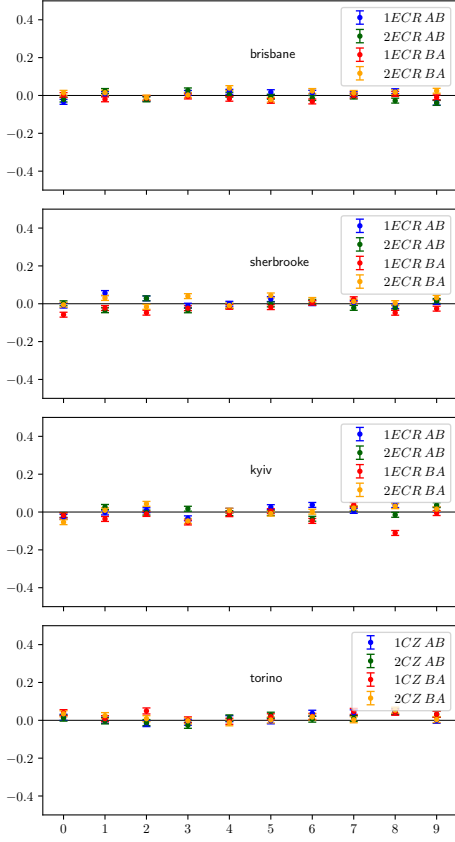


FIG. 17. Correlations $\langle \mathcal{AB} \rangle$ and $\langle \mathcal{BA} \rangle$ on the respective IBM devices. Description $nECR/CZ$ corresponds to $n = 1, 2$ ECR/CZ gate(s) in the protocol, while AB and BA correspond to the order $A \rightarrow B$ and $B \rightarrow A$. The solid lines are the perfect values 0.

For two weak ones, first $A \rightarrow B$ followed by C , we have

$$\begin{aligned}\langle \tilde{\mathcal{A}}\tilde{\mathcal{B}}\mathcal{C} \rangle &= \langle \mathcal{AC} \rangle - \langle \mathcal{AG}_B\mathcal{C} \rangle g_B, \\ \langle \tilde{\mathcal{A}}\mathcal{B}\mathcal{C} \rangle &= \langle \mathcal{BC} \rangle - \langle \mathcal{GA}\mathcal{B}\mathcal{C} \rangle g_A, \\ \langle \tilde{\mathcal{A}}\tilde{\mathcal{B}}\tilde{\mathcal{C}} \rangle &= \langle \mathcal{C} \rangle - \langle (\mathcal{GA}\mathcal{G}_A + \mathcal{GB}\mathcal{G}_B)\mathcal{C} \rangle + \langle \mathcal{GA}\mathcal{G}_B\mathcal{C} \rangle g_A g_B,\end{aligned}\quad (\text{B10})$$

Here \tilde{O} means that O is measured with ignored outcomes, so it may affect other observables.

Appendix C: IBM Quantum circuits

The default measured observable Z , can be changed $Z \rightarrow U^\dagger Z U$ by rotation U on the qubit,

$$X = Y_+ Z Y_-, \quad Y = X_- Z X_+ \quad (\text{C1})$$

expressed by native gates $Y_\pm = Z_\pm X_\mp$ and $X_- = Z X_+ Z$. We shall also use X rotated by $\pm\pi/4$ about Z axis, i.e.

$$X^\pm = Z_{\pm\pi/4} X Z_{\mp\pi/4} = (X \pm Y)/\sqrt{2} \quad (\text{C2})$$

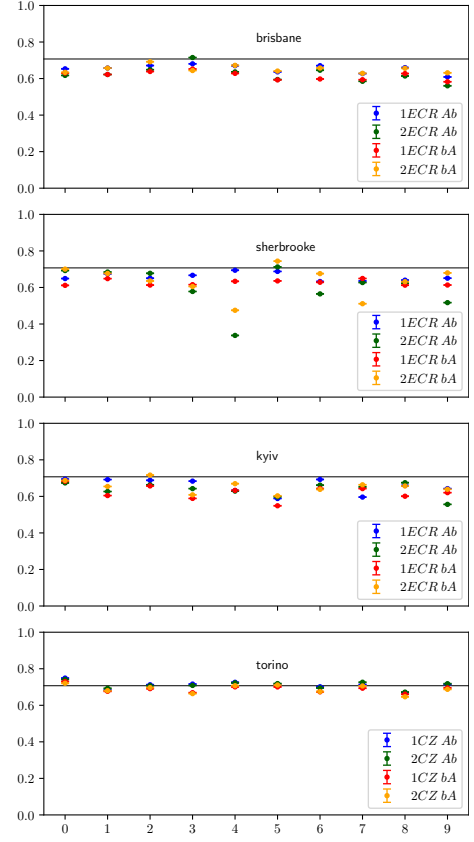


FIG. 18. Averages $\langle \mathcal{A} \rangle$ on the respective IBM devices. Description $nECR/CZ$ corresponds to $n = 1, 2$ ECR/CZ gate(s) in the protocol, while Ab and bA correspond to the order $A \rightarrow B$ and $B \rightarrow A$. The solid line is the perfect value $1/\sqrt{2}$.

to get $A = X^-$, $B = X^+$, $C = Z$. The initial state is obtained by $|\psi\rangle = Y_+|0\rangle$. Then $[A, B] = [X^-, X^+] = iZ$ and $[Z, Y] = -iX$ but $\rho = |\psi\rangle\langle\psi|$ is its eigenstate, so

$$\begin{aligned}\langle \mathcal{C} \rangle &= 0, \\ \langle \mathcal{A} \rangle &= \langle \mathcal{B} \rangle = 1/\sqrt{2}, \\ \langle \mathcal{AB} \rangle &= \langle \mathcal{BA} \rangle = 0, \\ \langle \mathcal{BC} \rangle &= 1/\sqrt{2} = -\langle \mathcal{AC} \rangle, \\ \langle \mathcal{ABC} \rangle &= 1/2 = -\langle \mathcal{BAC} \rangle\end{aligned}\quad (\text{C3})$$

Now the LG inequalities should be violated

$$\langle \mathcal{A} \rangle + \langle \mathcal{B} \rangle - \langle \mathcal{AB} \rangle = \sqrt{2} \quad (\text{C4})$$

but also

$$\begin{aligned}\langle \mathcal{A} \rangle + \langle \mathcal{C} \rangle - \langle \mathcal{AC} \rangle &= \sqrt{2}, \\ \langle \mathcal{B} \rangle - \langle \mathcal{C} \rangle + \langle \mathcal{BC} \rangle &= \sqrt{2},\end{aligned}\quad (\text{C5})$$

which can be reduced to (21) replacing C by B or $-A$.

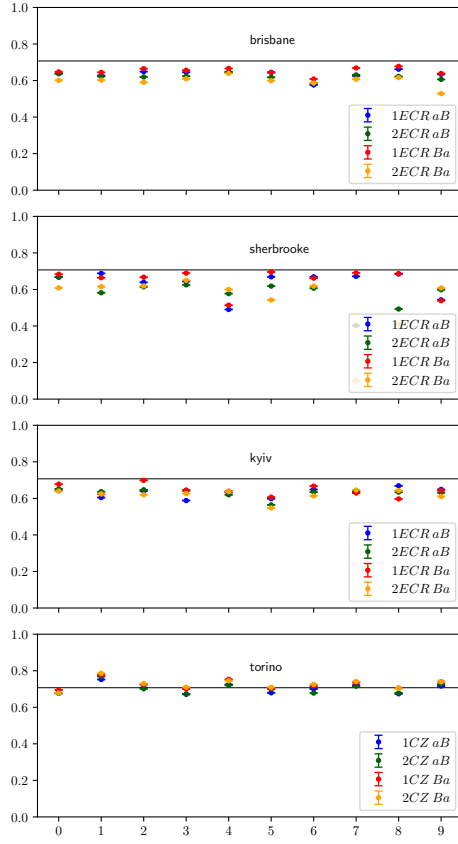


FIG. 19. Averages $\langle \mathcal{B} \rangle$ on the respective IBM devices. Description $nECR/CZ$ corresponds to $n = 1, 2$ ECR/CZ gate(s) in the protocol, while aB and Ba correspond to the order $A \rightarrow B$ and $B \rightarrow A$. The solid line is the perfect value $1/\sqrt{2}$.

Appendix D: Corrections from finite strength

To find corrections of finite invasiveness to the measurement $A \rightarrow B \rightarrow C$, we note that $\mathcal{G}_B C = -2\sqrt{2}A$, $\mathcal{G}_A C = 2\sqrt{2}B$, $\mathcal{G}_A B = 4B$, so

$$\begin{aligned} \langle \mathcal{A}\tilde{\mathcal{B}}C \rangle &= -1/\sqrt{2} + 2\sqrt{2}g_B, \\ \langle \tilde{\mathcal{A}}\mathcal{B}C \rangle &= 1/\sqrt{2}, \\ \langle \tilde{\mathcal{A}}\tilde{\mathcal{B}}C \rangle &= 2(g_B - g_A), \\ \langle \tilde{\mathcal{A}}\mathcal{B} \rangle &= 1/\sqrt{2} - 2\sqrt{2}g_A \end{aligned} \quad (D1)$$

For $B \rightarrow A \rightarrow C$ we get $\mathcal{G}_B A = 4A$, and so

$$\begin{aligned} \langle \mathcal{B}\tilde{\mathcal{A}}C \rangle &= 1/\sqrt{2} - 2\sqrt{2}g_A, \\ \langle \tilde{\mathcal{B}}\mathcal{A}C \rangle &= -1/\sqrt{2}, \\ \langle \tilde{\mathcal{B}}\tilde{\mathcal{A}}C \rangle &= 2(g_B - g_A), \\ \langle \tilde{\mathcal{B}}\mathcal{A} \rangle &= 1/\sqrt{2} - 2\sqrt{2}g_B. \end{aligned} \quad (D2)$$

Strong measurements $g = 1/4$ end up with highly disturbed results for $A \rightarrow B \rightarrow C$,

$$\langle \mathcal{A}\tilde{\mathcal{B}}C \rangle = \langle \tilde{\mathcal{A}}\mathcal{B} \rangle = 0 \quad (D3)$$

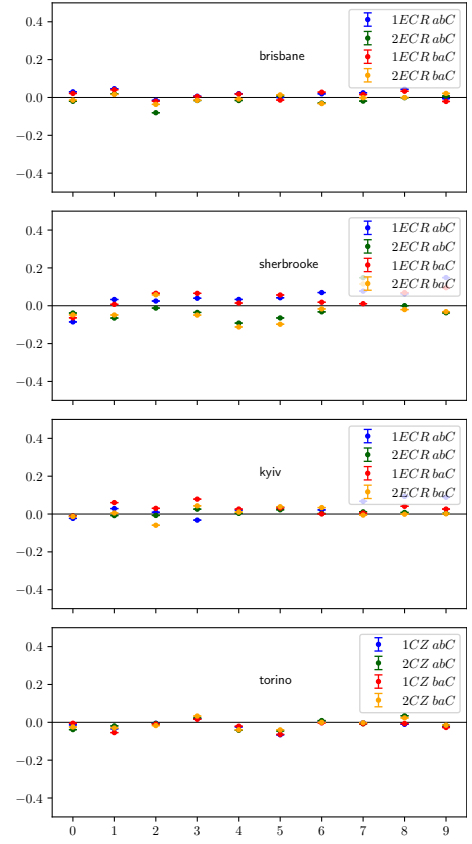


FIG. 20. Averages $\langle \mathcal{C} \rangle$ on the respective IBM devices. Description $nECR/CZ$ corresponds to $n = 1, 2$ ECR/CZ gate(s) in the protocol, while ab and ba correspond to the order $A \rightarrow B$ and $B \rightarrow A$. The solid line is the perfect value 0.

and for $B \rightarrow A \rightarrow C$,

$$\langle \mathcal{B}\tilde{\mathcal{A}}C \rangle = \langle \tilde{\mathcal{B}}\mathcal{A} \rangle = 0 \quad (D4)$$

The special case is $\langle \tilde{\mathcal{B}}\tilde{\mathcal{A}}C \rangle = \langle \tilde{\mathcal{A}}\tilde{\mathcal{B}}C \rangle$ which remain 0 for equal strength but bounds $1/2$ projection on A and weak measurement of B and $-1/2$ vice versa.

Appendix E: Full results of the test

Our tests allow to extract all averages and correlations, presented in Figs. 14, 17, 15, 16, 18, 19, 20. These results, except $\langle \mathcal{A}\mathcal{B} \rangle$, $\langle \mathcal{A}\mathcal{B}C \rangle$ and $A \leftrightarrow B$, differ clearly from projective measurements, confirming again the weak measurement regime. They roughly agree with the theoretical predictions.

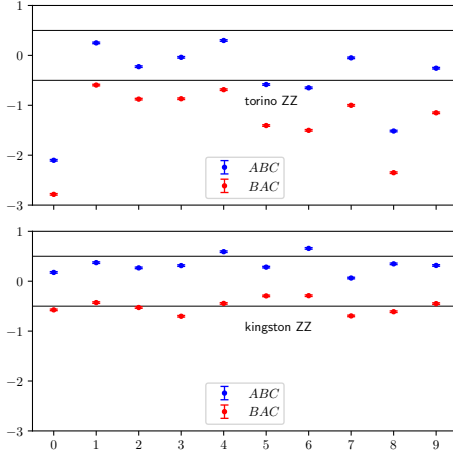


FIG. 21. Correlations $\langle ABC \rangle$ and $\langle BAC \rangle$ `ibm_torino` and `ibm_kingston` with RZZ gates. Here AB and BA correspond to the order $A \rightarrow B$ and $B \rightarrow A$. The solid lines are the perfect values ± 0.5 .

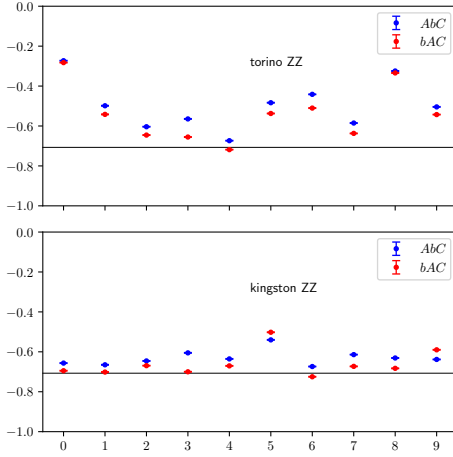


FIG. 22. Correlations $\langle AC \rangle$ `ibm_torino` and `ibm_kingston` with RZZ gates. Here AbC and bAC correspond to the order $A \rightarrow B$ and $B \rightarrow A$. The solid line is the perfect value $-1/\sqrt{2}$.

-
- [1] A. Einstein, B. Podolsky, N. Rosen, Can Quantum-Mechanical Description of Physical Reality Be Considered Complete?, *Phys. Rev.* **47**, 777 (1935).
 - [2] J.S. Bell, On the Einstein Podolsky Rosen paradox, *Physics* (Long Island City, N.Y.) **1**, 195 (1964); A. Shimony, Bell's Theorem, plato.stanford.edu/entries/bell-theorem/.
 - [3] J.F. Clauser, M.A. Horne, A. Shimony and R.A. Holt, Proposed Experiment to Test Local Hidden-Variable Theories *Phys. Rev. Lett.* **23**, 880(1969).
 - [4] N.D. Mermin, *Is the Moon There When Nobody Looks? Reality and the Quantum Theory*, *Phys. Today* **4**, 38 (1985).
 - [5] E.P. Wigner, *Phys. Rev.* **40** 749 (1932); M. Hillery, R. F. O'Connell, M. O. Scully and E. P. Wigner, *Phys. Rep.* **106**, 121 (1984); W.P. Schleich, *Quantum Optics in Phase Space*, (Wiley-VCH, Weinheim, 2001).
 - [6] E.C.G. Sudarshan, B. Misra, The Zeno's paradox in quantum theory, *J. Math. Phys.* **18**, 756 (1977).
 - [7] A. C. Elitzur and L. Vaidman, Quantum mechanical interaction-free measurements, *Found. Phys.* **23**, 987 (1993).
 - [8] C. Robens, W. Alt, C. Emary, D. Meschede, and A. Alberti, Atomic "bomb testing": the Elitzur-Vaidman experiment violates the Leggett-Garg inequality, *Appl. Phys. B* **123**, 12 (2017)
 - [9] A. J. Leggett and A. Garg, *Quantum mechanics versus macroscopic realism: Is the flux there when nobody looks?*, *Phys. Rev. Lett.* **54**, 857 (1985).
 - [10] C. Emary, N. Lambert, F. Nori, *Leggett-Garg inequalities*, *Rep. Prog. Phys.* **77**, 016001 (2014).

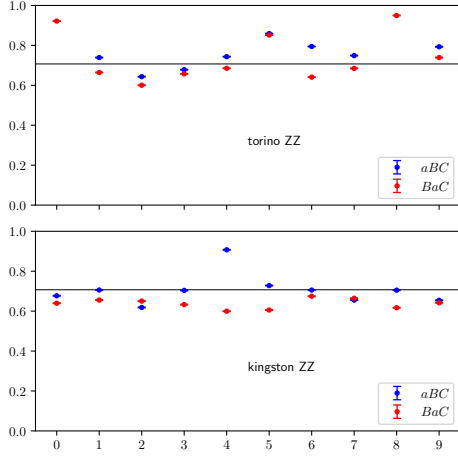


FIG. 23. Correlations $\langle BC \rangle$ on `ibm_torino` and `ibm_kingston` with RZZ gates. Here aBC and BaC correspond to the order $A \rightarrow B$ and $B \rightarrow A$. The solid lines are the perfect values $1/\sqrt{2}$.

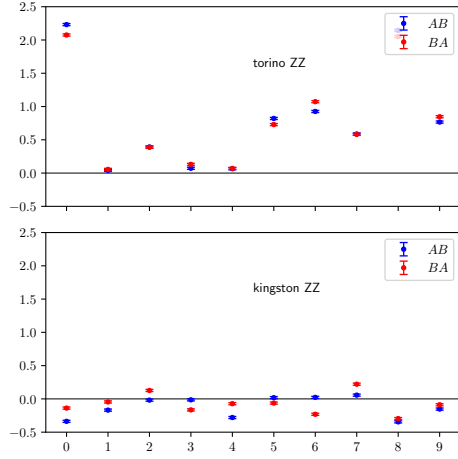


FIG. 24. Correlations $\langle AB \rangle$ and $\langle BA \rangle$ on `ibm_torino` and `ibm_kingston` with RZZ gates. Here AB and BA correspond to the order $A \rightarrow B$ and $B \rightarrow A$. The solid lines are the perfect values 0.

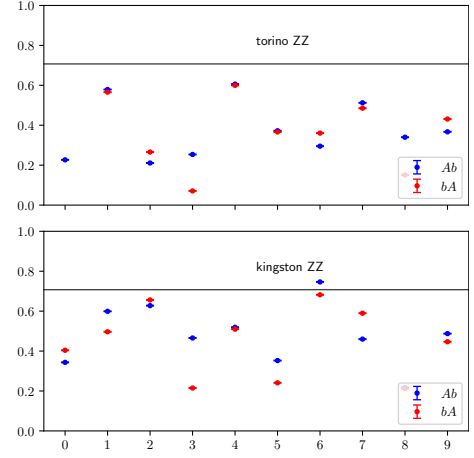


FIG. 25. Averages $\langle A \rangle$ on `ibm_torino` and `ibm_kingston` with RZZ gates. Here Ab and bA correspond to the order $A \rightarrow B$ and $B \rightarrow A$. The solid lines is the perfect value $1/\sqrt{2}$.

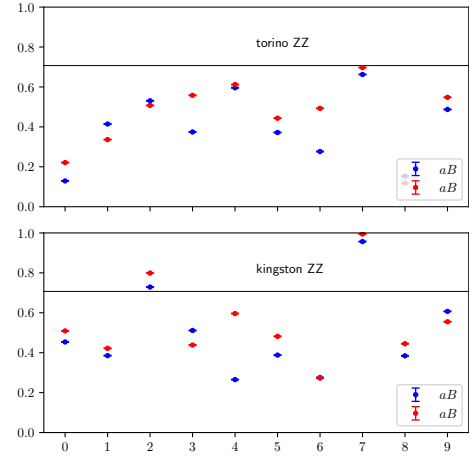


FIG. 26. Averages $\langle B \rangle$ on `ibm_torino` and `ibm_kingston` with RZZ gates. Here aB and Ba correspond to the order $A \rightarrow B$ and $B \rightarrow A$. The solid lines is the perfect value $1/\sqrt{2}$.

[11] J. von Neumann, *Mathematical Foundations of Quantum Mechanics* (Princeton University Press, Princeton, 1932).
[12] George C. Knee, Stephanie Simmons, Erik M. Gauger, John J. L. Morton, Helge Riemann, Nikolai V. Abrosimov, Peter Becker, Hans-Joachim Pohl, Kohei M. Itoh, Mike L. W. Thewalt, G. Andrew D. Briggs, Simon C. Benjamin, Violation of a Leggett-Garg inequality with ideal non-invasive measurements, *Nat. Commun.* 3, 606 (2012)
[13] C. Robens, W. Alt, D. Meschede, C. Emary, A. Alberti, Ideal negative measurements in quantum walks disprove theories based on classical trajectories, *Phys. Rev. X* 5, 011003 (2015)
[14] K. Kraus, *States, Effects and Operations* (Springer, Berlin, 1983).
[15] A. Peres, *Quantum Theory – Concept and Methods*, (Kluwer, Dordrecht, 2002)

[16] H. M. Wiseman and G. J. Milburn, *Quantum Measurement and Control* (Cambridge University Press, Cambridge, 2009).
[17] M. Nielsen, I. Chuang, *Quantum Computation and Quantum Information*, Cambridge University Press, 2010.
[18] G.C. Ghirardi, A. Rimini, T. Weber, Unified dynamics for microscopic and macroscopic systems, *Physical Review D* 34, 470 (1986)
[19] G. C. Ghirardi P. Pearle, A. Rimini, Markov processes in Hilbert space and continuous spontaneous localization of systems of identical particles, *Phys. Rev. A* 42, 78 (1990).
[20] P. Busch, "No information without disturbance": quantum limitations of measurement, in: *Quantum Reality, Relativistic Causality, and Closing the Epistemic Circle*, The Western Ontario Series in Philosophy of Science v. 73, eds. W. C. Myrvold and J. Christian (Springer, Dordrecht, 2009) p. 229

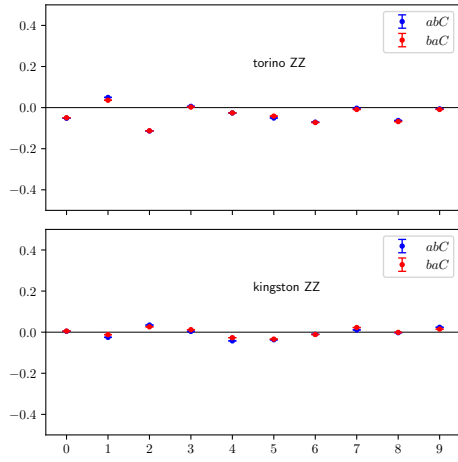


FIG. 27. Averages $\langle C \rangle$ on `ibm_torino` and `ibm_kingston` with RZZ gates. Here ab and ba correspond to the order $A \rightarrow B$ and $B \rightarrow A$. The solid line is the perfect value 0.

- [21] Y. Aharonov, D.Z. Albert, and L. Vaidman, *How the result of a measurement of a component of the spin of a spin-1/2 particle can turn out to be 100*, Phys. Rev. Lett. **60**, 1351 (1988).
- [22] N.W.M. Ritchie, J.G. Story, R.G. Hulet, Realization of a measurement of a "weak value", Phys. Rev. Lett. **66**, 1107 (1991).
- [23] A. C. Martinez-Becerril, G. Bussieres, D. Curic, L.Giner, R. A. Abrahao, J. S. Lundeen, Theory and experiment for resource-efficient joint weak-measurement, Quantum **5**, 599 (2021)
- [24] J. S. Lundeen, B. Sutherland, A. Patel, C. Stewart, C. Bamber, Direct Measurement of the Quantum Wavefunction, Nature, **474**, 188 (2011)
- [25] E. Rebufello, F. Piacentini, A. Avella, M. A. de Souza, M. Gramegna, J. Dziewior, E. Cohen, L. Vaidman, I. P. Degiovanni, M. Genovese, Anomalous weak values via a single photon detection, Light: Science & Applications **10**, 106 (2021)
- [26] Yosep Kim, Dong-Gil Im, Yong-Su Kim, Sang-Wook Han, Sung Moon, Yoon-Ho Kim, Young-Wook Cho, Observing the quantum Cheshire cat effect with noninvasive weak measurement, npj Quantum Inf **7**, 13 (2021)
- [27] R. Ruskov, A. N. Korotkov, and A. Mizel, Signatures of Quantum Behavior in Single-Qubit Weak Measurements, Phys. Rev. Lett. **96**, 200404 (2006).
- [28] Y. Suzuki, M. Iinuma, and H. F. Hofmann, Violation of Leggett-Garg inequalities in quantum measurements with variable resolution and back-action, New J. Phys. **14**, 103022 (2012).
- [29] A. Palacios-Laloy, F. Mallet, F. Nguyen, P. Bertet, D. Vion, D. Esteve, and A.N. Korotkov, *Experimental violation of a Bell's inequality in time with weak measurement*, Nat. Phys. **6**, 442 (2010).
- [30] A. N. Jordan, A. N. Korotkov, and M. Büttiker, Leggett-Garg Inequality with a Kicked Quantum Pump, Phys. Rev. Lett. **97**, 026805 (2006).
- [31] N. S. Williams and A. N. Jordan, Weak Values and the Leggett-Garg Inequality in Solid-State Qubits, Phys. Rev. Lett. **100**, 026804 (2008).
- [32] M.E. Goggin, M.P. Almeida, M. Barbieri, B.P. Lanyon, J.L. O'Brien, A.G. White, G.J. Pryde, Violation of the Leggett-Garg inequality with weak measurements of photons, Proc. Natl. Acad. Sci. U.S.A. **108**, 1256, <https://doi.org/10.1073/pnas.1005774108> (2011).
- [33] Alessio Avella, Fabrizio Piacentini, Michelangelo Borsarelli, Marco Barbieri, Marco Gramegna, Rudi Lussana, Federica Villa, Alberto Tosi, Ivo Pietro Degiovanni, and Marco Genovese, Anomalous weak values and the violation of a multiple-measurement Leggett-Garg inequality, Phys. Rev. A **96**, 052123 (2017)
- [34] J. Dressel, C. J. Broadbent, J. C. Howell, and A. N. Jordan, Experimental violation of Two-Party Leggett-Garg Inequalities with Semiweak Measurements, Phys. Rev. Lett. **106**, 040402 (2011)
- [35] Justin Dressel and Alexander N. Korotkov, Avoiding loopholes with hybrid Bell-Leggett-Garg inequalities, Phys. Rev. A **89**, 012125 (2014).
- [36] T. C. White, J.Y. Mutus, J. Dressel, J. Kelly, R. Barends, E. Jeffrey, D. Sank, A. Megrant, B. Campbell, Y. Chen, et al. Preserving entanglement during weak measurement demonstrated with a violation of the Bell-Leggett-Garg inequality. npj Quantum Information **2**, 1 (2016).
- [37] A. Bednorz and W. Belzig, *Quasiprobabilistic Interpretation of Weak Measurements in Mesoscopic Junctions*, Phys. Rev. Lett. **105**, 106803 (2010).
- [38] A. Bednorz, W. Belzig, A. Nitzan, Nonclassical time correlation functions in continuous quantum measurement, New J. Phys. **14**, 013009 (2012)
- [39] A. Bednorz, K. Franke, W. Belzig, *Noninvasiveness and time symmetry of weak measurements*, New J. Phys. **15**, 023043 (2013).
- [40] D. Curic, M. C. Richardson, G. S. Thekkadath, J. Florez, L. Giner, and J. S. Lundeen, *Experimental investigation of measurement-induced disturbance and time symmetry in quantum physics*, Phys. Rev. A **97**, 042128 (2018).
- [41] S.Soltan, M. Frączak, W. Belzig, A. Bednorz, Conservation laws in quantum noninvasive measurements, Phys. Rev. Research **3**, 013247 (2021).
- [42] IBM Quantum Platform, quantum.ibm.com
- [43] <https://qiskit.org/textbook>
- [44] E. Huffman, A. Mizel, Leggett-Garg test of superconducting qubit addressing the clumsiness loophole Phys. Rev. A **95**, 032131 (2017)
- [45] A. Santini, V. Vitale, Experimental violations of Leggett-Garg's inequalities on a quantum computer, Phys. Rev. A **105**, 032610 (2022)
- [46] D. R. A. Ruelas Paredes, M. Uria, Eduardo Massoni, Francisco De Zela, Testing precision and accuracy of weak value measurements in an IBM quantum system, AVS Quantum Sci. **6**, 015001 (2024)
- [47] <https://www.ibm.com/quantum/blog/fractional-gates>
- [48] D. Bures, Trans. Amer. Math. Soc. **135**, 199 (1969)
- [49] S.D. Bartlett, T. Rudolph, R.W. Spekkens, *Reference frames, superselection rules, and quantum information*, Rev. Mod. Phys. **79**, 555 (2007).
- [50] A. Bednorz, C. Bruder, B. Reulet, and W. Belzig, Phys. Rev. Lett. **110**, 250404 (2013)
- [51] J. Bülte, A. Bednorz, C. Bruder, and W. Belzig, *Noninvasive Quantum Measurement of Arbitrary Operator Order by Engineered Non-Markovian Detectors*, Phys. Rev. Lett. **120**, 140407 (2018).
- [52] T.C. Ralph, S.D. Bartlett, J.L. O'Brien, G.J. Pryde, H.M. Wiseman, Quantum nondemolition measurements

- for quantum information, Phys. Rev. A **73**, 012113 (2006).
- [53] G.J. Pryde, J.L. O'Brien, A.G. White, S.D. Bartlett, T.C. Ralph, Measuring a photonic qubit without destroying it, Phys. Rev. Lett. **92**, 190402 (2004).
 - [54] G.J. Pryde, J.L. O'Brien, A.G. White, T.C. Ralph, H.M. Wiseman, Measurement of quantum weak values of photon polarization, Phys. Rev. Lett. **94**, 220405 (2005).
 - [55] J. Koch, T. M. Yu, J. Gambetta, A. A. Houck, D. I. Schuster, J. Majer, A. Blais, M. H. Devoret, S. M. Girvin, R. J. Schoelkopf, Charge-insensitive qubit design derived from the Cooper pair box, Phys. Rev. A **76**, 042319 (2007).
 - [56] J. M. Gambetta, J. M. Chow, and M. Steffen, *Building logical qubits in a superconducting quantum computing system* npj Quantum Inf. **3**, 2 (2017).
 - [57] P. Krantz, M. Kjaergaard, F. Yan, T.P. Orlando, S. Gustavsson, and W.D. Oliver, A quantum engineer's guide to superconducting qubits, Appl. Phys. Rev. **6**, 021318 (2019).
 - [58] T. Alexander, N. Kanazawa, D. J. Egger, L. Capelluto, C. J. Wood, A. Javadi-Abhari, and D. C. McKay, Qiskit pulse: programming quantum computers through the cloud with pulses, Quantum Sci. Technol. **5**, 044006 (2020).
 - [59] K. X. Wei, E. Magesan, I. Lauer, S. Srinivasan, D. F. Bogorin, S. Carnevale, G. A. Keefe, Y. Kim, D. Klaus, W. Landers, N. Sundaresan, C. Wang, E. J. Zhang, M. Steffen, O. E. Dial, D. C. McKay, A. Kandala, Quantum crosstalk cancellation for fast entangling gates and improved multi-qubit performance Phys. Rev. Lett. **129**, 060501 (2022)
 - [60] M. Malekakhlagh, E. Magesan, and D. C. McKay, First-principles analysis of cross-resonance gate operation, Phys. Rev. A **102**, 042605 (2020).
 - [61] E. Magesan and J. M. Gambetta, Effective Hamiltonian models of the cross-resonance gate, Phys. Rev. A **101**, 052308 (2020).
 - [62] IonQ documentation, docs.ionq.com
 - [63] C. Figgatt, Building and Programming a Universal Ion Trap Quantum Computer, PhD thesis, 2018, duke.app.box.com/s/l5xqv2njo06avkow2rl0jqz5165946ah
 - [64] K. Wright, Manipulation of the Quantum Motion of Trapped Atomic Ions via Stimulated Raman Transitions, PhD Thesis 2017, duke.app.box.com/s/qy7yalogjwkc84lzy1urr4q556opwhh
 - [65] L. Egan, Scaling Quantum Computers with Long Chains of Trapped Ions, PhD thesis 2021, duke.app.box.com/s/1t8vdf34v60rgso101d8fpjmptl752ch
 - [66] S. Debnath, A Programmable Five Qubit Quantum Computer using Trapped Atomic Ions, PhD thesis 2016, duke.app.box.com/s/b7hr7z069q4bddgo8ep3w2f1avphy368
 - [67] K. Landsman, Construction, Optimization, and Applications of a Small Trapped-Ion Quantum Computer, PhD thesis 2019, duke.app.box.com/s/qigghzotrws9fiqgmo6i7e6gvjvrek9p
 - [68] G. N. Nop, D. Paudyal, and J. D. H. Smith, Ytterbium ion trap quantum computing: The current state-of-the-art, AVS Quantum Sci. **3**, 044101 (2021)
 - [69] European Organization For Nuclear Research and Open AIRE, Zenodo, CERN, 2021, <https://doi.org/10.5281/zenodo.16402161>